Structure
Article

The Crystal Structure of the Extracellular 11-heme Cytochrome UndA Reveals a Conserved 10-heme Motif and Defined Binding Site for Soluble Iron Chelates

Marcus J. Edwards,[1] Andrea Hall,[1] Liang Shi,[2] James K. Fredrickson,[2] John M. Zachara,[2] Julea N. Butt,[1] David J. Richardson,[1,*] and Thomas A. Clarke[1,*]
[1]Centre for Molecular and Structural Biochemistry, School of Biological Sciences and School of Chemistry, University of East Anglia, Norwich Research Park, Norwich NR4 7TJ, UK
[2]Pacific Northwest National Laboratory, Richland, WA 99352, USA
*Correspondence: d.richardson@uea.ac.uk (D.J.R.), tom.clarke@uea.ac.uk (T.A.C.)
DOI 10.1016/j.str.2012.04.016

SUMMARY

Members of the genus *Shewanella* translocate deca- or undeca-heme cytochromes to the external cell surface thus enabling respiration using extracellular minerals and polynuclear Fe(III) chelates. The high resolution structure of the first undeca-heme outer membrane cytochrome, UndA, reveals a crossed heme chain with four potential electron ingress/egress sites arranged within four domains. Sequence and structural alignment of UndA and the deca-heme MtrF reveals the extra heme of UndA is inserted between MtrF hemes 6 and 7. The remaining UndA hemes can be superposed over the heme chain of the decaheme MtrF, suggesting that a ten heme core is conserved between outer membrane cytochromes. The UndA structure has also been crystallographically resolved in complex with substrates, an Fe(III)-nitrilotriacetate dimer or an Fe(III)-citrate trimer. The structural resolution of these UndA-Fe(III)-chelate complexes provides a rationale for previous kinetic measurements on UndA and other outer membrane cytochromes.

INTRODUCTION

Bacteria from the genus *Shewanella* can respire using extracellular minerals and soluble iron chelates as terminal electron acceptors. These respiratory processes influence the speciation of essential transition metals such as iron and manganese, and can be exploited in the engineering of microbial fuel cells. The surfaces of mineral respiring *Shewanella* can contain different solvent-exposed multiheme cytochromes that have been implicated in the extracellular electron transfer to various soluble and solid-phase electron acceptors (Lower et al., 2007, 2009). The most commonly studied are the three outer membrane cytochromes (OMC) from *Shewanella oneidensis*, namely the decaheme cytochromes MtrC (Hartshorne et al., 2007), MtrF (McLean et al., 2008), and OmcA (Ross et al., 2009; Xiong et al., 2006) that are encoded by a metal reducing (mtr) gene cluster, *mtrDEF-omcA-mtrCAB*.

Analysis of the metal reducing loci from multiple *Shewanella* genomes revealed that other mineral-reductase clusters contain the genes for a number of different OMC (Fredrickson et al., 2008). In addition to MtrC, MtrF, and OmcA, genes encoding the decaheme cytochromes MtrG and MtrH, and the 11-heme cytochromes UndA and UndB, were also identified. This comparative genomic analysis revealed that the 11-heme cytochrome UndA substitutes for OmcA in a number of *Shewanella* species (Fredrickson et al., 2008). A recent study into the *Shewanella* community associated with near-shore sediments from the Columbia River along the Hanford Reach (Washington, USA) resulted in the isolation of 23 different *Shewanella* strains. Out of seven strains tested, UndA was found to have substituted for OmcA in four, demonstrating that these 11-heme OMCs are widely dispersed throughout the *Shewanella* family (Shi et al., 2011).

The complex formed by the gene products of the *mtrCAB* cluster has been biochemically characterized. The MtrC cytochrome is located on the surface of the outer membrane and associates with the 28 β strand transmembrane porin MtrB (Beliaev and Saffarini, 1998). The MtrB porin also associates with the periplasmic decaheme cytochrome MtrA (Pitts et al., 2003), forming a stable 20-heme transmembrane complex that facilitates electron transfer across the outer membrane from the periplasm to the cell surface. MtrB functions as a sheath that positions MtrC and MtrA in a configuration that allows direct electron transfer between both cytochromes (Hartshorne et al., 2009). A similar complex may be formed by MtrF, MtrD, and MtrE, where MtrE is a 28 β strand transmembrane porin that facilitates electron transfer between the periplasmic MtrD and cell-surface MtrF across the outer membrane (Clarke et al., 2011).

The *omcA* gene lies between the *mtrDEF* and *mtrCAB* genes, but is part of a separate operon. However, OmcA has been shown to associate with the MtrCAB complex, suggesting that it may accept electrons from MtrC, before transfer to terminal extracellular electron acceptors (Ross et al., 2007; Shi et al., 2006). It has therefore been proposed that OmcA has a supportive role in reduction, including being involved with binding of *S. oneidensis* to mineral oxides, as well as assisting in electron transfer (Coursolle et al., 2010). As the *undA gene* is

a homolog of *omcA*, it is likely that UndA will also have a supportive reductive role to the MtrCAB complex.

A recent study showed that MtrC, OmcA, and MtrF have overlapping roles, but that MtrC is the predominant cytochrome involved in mineral reduction (Coursolle and Gralnick, 2010). These overlapping roles are rationalized through studies where the rates of ferrous cytochrome oxidation after mixing with substrate were used to obtain second-order rate constants for the reduction of the soluble electron acceptors Fe(III)-citrate, Fe(III)-nitrilotriacetate (Fe(III)-NTA), and Fe(III)-EDTA (Ross et al., 2009; Wang et al., 2008). Under these conditions, the addition of insoluble minerals such as goethite results in a very low rate of cytochrome oxidation, leading to arguments that these OMC do not directly interact with insoluble iron oxides, instead relying on soluble electron shuttles such as flavin mononucleotide (FMN) to mediate electron transfer (Ross et al., 2009). Although the second order rate constants measured for Fe(III)-chelate oxidation were physiologically relevant, the rate of reduction of Fe(III)-citrate by MtrC or OmcA was significantly slower than either Fe(III)-NTA or Fe(III)-EDTA. In addition, the observed rates could also be biphasic, most notably for Fe(III) citrate. UndA was capable of reducing Fe(III)-citrate or Fe(III)-NTA at rates greater than or similar to MtrC or OmcA (Ross et al., 2009; Shi et al., 2011), whereas reduction of Fe(III)-EDTA occurred at rates greater than ten times that observed for either OmcA or MtrC.

The observed rate constants can be affected by a number of factors, including the interaction between Fe(III)-chelate and cytochrome, the structure of the Fe(III)-chelate, as well as the reorganization energy and differences in the electrochemical potentials between the different hemes and electron donors. Fe(III)-EDTA is the simplest, and forms a ferric ion-ligand complex with a 1:1 stoichiometry, whereas Fe(III)-citrate and Fe(II)-NTA form a range of higher order complexes depending on concentration and Fe(III): chelate ratio. The most physiologically relevant of these chelates is citrate that is abundant in the natural environment, NTA often occurs in sewage and contaminated waters, whereas EDTA is rarely found outside of an industrial setting.

In contrast to the understanding of OMC oxidation kinetics, the structures of OMC that form the interface between the cell surface and extracellular terminal electron acceptor are poorly characterized. The only published structure of an OMC is of the MtrC paralog MtrF, which was resolved to 3.2 Å. The MtrF is comprised of four domains. Two β-barrel domains flank two pentaheme domains that associate to form a heme chain consisting of a total of ten *bis*-histidine coordinated *c*-type hemes arranged in a "staggered cross" conformation that spans the structure (Clarke et al., 2011). The β-barrel domains may either form binding sites for soluble redox substrates, or provide support to the overall decaheme structure. To date there is no structure with substrate bound available for any OMC, and no molecular structural detail for MtrA. A low resolution surface map of OmcA obtained through small-angle X-ray scattering suggested that OmcA has a flat ellipsoidal shape similar to MtrF (Johs et al., 2010). There is often conservation of heme packing motifs within different families, the arrangement of hemes within the multiheme cytochromes NrfA, TvNIR, and HAO are very highly conserved, despite existing in different bacteria and having different functions. The staggered cross motif of ten hemes in MtrF is significantly different from any known multiheme cytochrome family (Sharma et al., 2010). The branched heme wire of MtrF contains multiple potential electron ingress/egress sites, suggesting a multitude of ways for electrons to interact with MtrF (Clarke et al., 2011).

We present here the crystal structure of UndA isolated from *Shewanella* sp. strain HRCR-6, which is, to our knowledge, the first example of an 11-heme OMC. We also present this structure in complex with the Fe(III) chelates Fe(III)-citrate and Fe(III)-NTA. This high resolution structure of an 11-heme OMC provides evidence that both Fe(III)-citrate and Fe(III)-NTA bind at discrete sites on UndA prior to reduction.

RESULTS

1.8 Å Crystal Structure of UndA

Crystals of UndA(HRCR-6) were prepared and diffraction data collected as described in Experimental Procedures. An initial model structure was built into an electron density map obtained by single-wavelength anomalous dispersion (SAD), using phases obtained from the anomalous iron signal to a resolution of 3.4 Å. This structure was then used as a model for molecular replacement into data collected to a final resolution of 1.76 Å. (Table 1). The UndA structure contained 11 *bis*-histidine coordinated *c*-type hemes and residues 44 to 843 of the polypeptide chain (Figure S1 available online). Electron density that could be attributed to two associated magnesium ions and one calcium ion was also identified on the surface of the UndA structure.

The molecular structure of the UndA protein has overall approximate dimensions of 90 × 70 × 50 Å and consists of a single peptide chain folded into four domains (Figure 1A). Domain I is a β-barrel domain containing a Cys_{165}-Cys_{169} disulfide bond and an extended pair of β strands that reach across the surface of the UndA structure; domain II is a pentaheme domain containing five of the *bis*-His coordinated c-type hemes; domain III is a second β-barrel domain containing a Cys_{599}-Cys_{615} disulfide bond; domain IV is a hexaheme domain containing the remaining six bis-His coordinated hemes. The four domains are arranged in a similar conformation to MtrF, with domain IV forming a contact with domains I and II (Figure 1A). The arrangement of the four domains results in a pseudo 2-fold symmetry axis between the two halves of UndA as indicated by the dashed line on Figure 1A. Superposition of the α-carbon atoms of domains I and II over domains III and IV gave an overall root-mean-square deviation (rmsd) of 3.9 Å whereas alignment of the amino acid sequences of the two UndA halves revealed a similarity of 23% between domains I, II and III, IV (Figure S2).

An 11-heme staggered cross consisting of a 70 Å 8-heme chain bisected by a 50 Å 5-heme chain is formed by pentaheme domain II and hexaheme domain IV (Figure 1B). All the heme porphyrin rings are within 6 Å of the nearest neighbor, allowing for rapid electron transfer across all 11 hemes (Figure 1B). The atoms of the UndA hemes can be superposed over the atoms of the MtrF hemes with an average rmsd of 3.7 Å (Table 2), revealing a core ten-heme staggered cross motif that is conserved between MtrF and UndA (Figure 1C). This conserved heme core also reveals that UndA heme 7 is the additional heme in UndA. Structure based alignment of the amino acid sequences

Table 1. Data Collection and Refinement Statistics for SAD and Molecular Replacement Data

	SAD	Native	Fe(III)-citrate	Fe(III)-NTA
Data collection				
Space group	$P2_12_12_1$	$P2_12_12_1$	$P2_12_12_1$	$P2_12_12_1$
Cell dimensions				
a, b, c (Å)	69.28, 105.92, 150.05	69.64, 106.09, 151.65	69.88, 106.53, 151.12	69.50, 105.87, 151.52
A, β, γ (°)	90.00, 90.00, 90.00	90.00, 90.00, 90.00	90.00, 90.00, 90.00	90.00, 90.00, 90.00
Wavelength (Å)	1.72	0.97	0.97	0.97
Resolution (Å)	62.9–3.4 (3.5–3.4)[a]	46.1–1.76 (1.81–1.76)	61.63–2.23 (2.29–2.23)	69.5–2.10 (2.16–2.10)
R_{sym} (%)	6.5 (9.5)	9.4 (33.2)	5.7 (36.5)	7.8 (37.8)
I/σI	9.8 (7.1)	4.8 (2.2)	11.7 (2.0)	9.1 (1.9)
Completeness (%)	97.6 (96.8)	99.8 (99.3)	99.1 (98.1)	99.5 (99.3)
Redundancy	20.5(19)	3.9 (3.7)	3.6 (3.6)	4.4 (4.3)
Refinement				
Resolution (Å)		1.76	2.23	2.10
No. reflections		105,111	52,335	62,231
R_{work}/R_{free}		0.14/0.18	0.16/0.21	0.16/0.20
No. atoms				
Protein		5,990	5,956	5,962
Ligand/ion		506	525	558
Water		1,318	828	996
B-factors				
Protein		21.3	35.1	24.47
Ligand/ion		17.4	27.9	22.07
Water		22.4	41.0	34.20
Rmsd				
Bond lengths (Å)		0.016	0.017	0.016

See also Figure S1.

[a]Values in parentheses are for highest-resolution shell. Rmsd, root-mean-square deviation; SAD, single-wavelength anomalous dispersion.

of UndA and MtrF shows that UndA heme 7 is part of a ~20 amino acid insertion between the distal histidine ligand and CXXCH motif of heme 7 in the corresponding MtrF amino acid sequence (Figure 2). The insertion of the oligopeptide containing heme 7 causes minimal disruption to the overall UndA structure, as hemes 6/8 of UndA and hemes 6/7 of MtrF and corresponding distal histidine ligands are superposable (Figure 3A).

The only other significant difference in the conformation of the other ten hemes is that of heme 5, where the propionates are rotated ~180° relative to that of MtrF and buried in the peptide fold of domain 2. This causes heme 5 of UndA to be much less exposed than MtrF heme, with relative solvent exposures of 161 $Å^2$ and 258 $Å^2$ for hemes 5 of UndA and MtrF, respectively (Figure 3B).

Overall the heme propionate groups in MtrF are solvent-exposed, giving a strong negative charge to one face of MtrF (Clarke et al., 2011) (Figure 4A). However, in UndA the negatively charged area is localized around heme 11 (Figure 4B). This is caused by insertions of polypeptide in the amino acid sequence of UndA that correspond to structural features that partially shield the surface of domains II and III of UndA (Figure 4C) so the average solvent accessibility of the UndA hemes is much lower than of MtrF (Table 2). Hemes 7 and 8 in UndA are arranged so that the propionate groups form a negatively charged pocket. This negative environment is compensated through hydrogen bonding to Lys_{712}, Arg_{716}, Arg_{732}, and Arg_{736}, resulting in an average overall positive charge on the surface of the pocket (Figure S3). The edge of the heme 7 porphyrin ring is also the most solvent accessible heme in the UndA structure with an exposed surface area of 207 $Å^2$. The imidazole side chains of the histidine ligands of *bis*-His coordinated heme-iron have either near-parallel or near-perpendicular orientation relative to each other, and most multi-heme cytochromes have a mixture of both. MtrF has six parallel histidine ligands and four perpendicular. In the pentaheme domain II of UndA, there are three parallel and two perpendicular histidine ligand pairs, whereas in the hexaheme domain IV all the histidine ligand pairs are perpendicular.

The cysteines of the disulfide bridges in the β-barrel domains I and III are mainly conserved in the sequences of the other OMC expressed by the *Shewanella* family (Figure 2). These motifs appear to stabilize short loop regions in the barrel domains for each protein. The improved resolution of UndA allows observation of the Cys_{165}-Cys_{169} in domain I, which is missing in the MtrF structure due to poor resolution and disorder in this region. The positions of the disulfide bonds in UndA cannot facilitate electron transfer to the hemes (distance >16 Å) so it is more likely that these disulfides are involved in stabilizing the β-barrel fold.

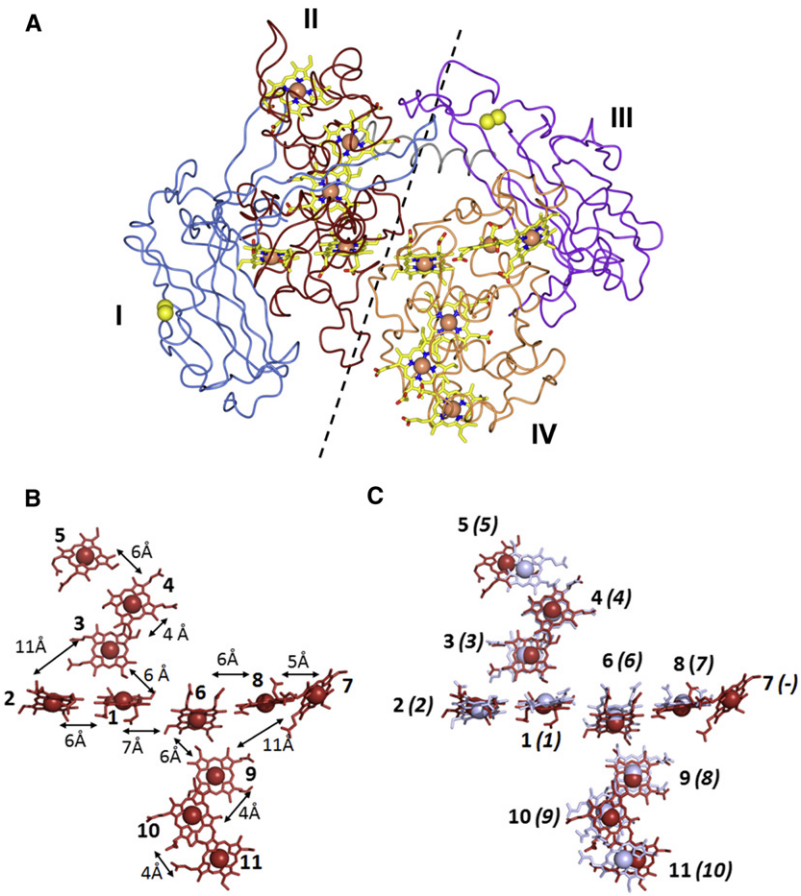

Figure 1. Structure of UndA

(A) Ribbon representation of the UndA crystal structure with the four domains colored (I) blue, (II) red, (III) purple, (IV) orange. The two disulfide bonds are colored as yellow spheres. The carbons atoms of the 11 *c*-type hemes are displayed as yellow sticks with the iron atoms shown as orange spheres. The pseudo 2-fold axis of symmetry of UndA is indicated by the dashed line.

(B) Arrangement of heme cofactors within UndA with distances between porphyrin rings shown. The hemes are displayed as sticks with the Fe atoms displayed as spheres and numbered according to the position of the corresponding CXXCH motif in the peptide sequence.

(C) Overlay of MtrF (blue) and UndA (red) heme cofactors. Hemes are numbered according to the position of the corresponding CXXCH motif in the peptide sequence, UndA heme numbers are in bold, MtrF heme numbers are in italicized parentheses.

See also Figure S2.

Interaction of UndA with Soluble Fe(III) Chelates

Putative UndA ligands were screened using crystals of UndA soaked in mother liquor containing ligand. Putative UndA ligands included the soluble Fe(III)-chelates Fe(III)-citrate, Fe(III)-NTA, and Fe(III)-EDTA. Saturating concentrations of the proposed electron shuttles flavin mononucleotide (FMN), riboflavin, FADH, and menaquinone were also used. UndA electron density maps were obtained for all conditions to final resolutions better than 2.4 Å, allowing for identification of ligands associated to UndA. The structure of UndA soaked with Fe(III)-EDTA did not contain additional electron density, suggesting that Fe(III)-EDTA did not associate with UndA under these conditions. In addition, no electron density was observed for any of the proposed electron shuttles.

F_o-F_c electron density maps, obtained from crystals soaked with Fe(III)-NTA for 10 min prior to harvesting, contained four sites with a σ-level over 8.5 that corresponded to two pairs of Fe^{3+} ions (Figure S4). Electron density surrounding the two Fe^{3+} ions was modeled as an oxo-bridged NTA ligand pair, giving two oxo-bridged Fe(III)-NTA dimers associated to UndA. The oxo-bridged NTA is an experimentally established arrangement for Fe(III)-NTA (Heath et al., 1992). One Fe(III)-NTA dimer is coordinated on the surface of UndA by Glu_{659} but is too far from the nearest heme to accept electrons (>16 Å). This association is therefore unlikely to be catalytically relevant (Figure 5A). The second Fe-NTA dimer associates with UndA near heme 7 through hydrogen bonds between two NTA carboxyl groups. The first NTA molecule binds to the guanidinium group of Arg_{528}, whereas the second binds to backbone amide groups of Ser_{710} and Lys_{711} (Figure 5B). This association would allow rapid electron transfer, with both Fe(III)-NTA iron atoms within 6.2– 8.3 Å of the heme 7 porphyrin ring (Figure 5D).

F_o-F_c maps, obtained from UndA crystals soaked with 10 mM Fe(III)-citrate for 10 min, prior to harvesting, contained three sites with σ-levels over 8.5. These sites were all within 3 Å of each other, indicating the presence of a single tri-iron ligand (Figures 5C and S5). The electron density surrounding these iron sites could be modeled to three citrate molecules, indicating that a single $Fe(III)_3$-$citrate_3$ complex had associated close to heme 7 of UndA (Figure 6B). This trimer associates to UndA through hydrogen bonding between Arg_{528} and carboxy groups from a single citrate molecule. This brings the three iron atoms of the Fe(III)-citrate trimer within 6.7–8.3 Å to the heme 7 porphyrin ring (Figure 5D).

The arrangement of the three irons and citrates is asymmetric, with two iron atoms coordinated by two carboxyl and two carbonyl groups from two citrates, and the third iron coordinated by a carboxyl, carbonyl and water. An oxo-bridge between the third and second iron completes the octahedral geometry of all three irons. This arrangement resembles a combination of previous models proposed for Fe(III)-citrate dimers and trimers (Silva et al., 2009), suggesting that the Fe(III)-citrate trimer assembles from a Fe(III)-citrate dimer (Figure 6).

DISCUSSION

The UndA structure presented here was solved at sufficient resolution to observe the binding of substrates to the polypeptide surface. The 11-heme UndA represents the largest known member of the *Shewanella* OMC family, whereas the previously published decaheme MtrF structure represents the smallest. The overall structural fold of UndA has significant homology to the previously published structure of MtrF, despite a sequence

Table 2. Comparison of UndA and MtrF Hemes

Heme Number (UndA/MtrF)	Rmsd[b] (Å)	Heme Area Exposed to Solvent[a]	
		UndA (Å^2)	MtrF (Å^2)
1/1	2.21	72.6	138
2/2	2.18	75.4	182
3/3	2.17	6.70	16.8
4/4	1.72	104	226
5/5	10.1	161	258
6/6	1.56	67.5	110
7	—	123	—
8/7	1.96	5.30	226
9/8	1.49	34.4	27.6
10/9	1.71	156	231
11/10	2.42	236	294

[a]The solvent exposure of each heme was calculated using CCP4: AREAIMOL[18].
[b]Heme atoms of MtrF were superposed over the corresponding heme atoms of UndA and overall rmsd calculated using CCP4: SUPERPOSE (Bailey, 1994). Rmsd, root-mean-square deviation.

identity of <24%, an additional 100 amino acids, and an extra heme. The similarity in overall domain and heme arrangement between UndA and MtrF structures suggests that all members of this outer membrane cytochrome family share a similar structure of a four domain fold that consists of two multiheme domains and two flanking β-barrel domains. Sequence alignments of MtrF and UndA with MtrC and OmcA support this proposal, indicating two penta-heme regions separated by regions that could fold into β-barrel structures containing conserved disulfides (Figure 2). The presence of the conserved cysteine pairs within the domains of MtrC and OmcA point toward stabilization of β strand hairpins as observed in the structures of MtrF and UndA and suggests these cytochromes are also likely to be composed of alternating β-barrel and multiheme cytochrome domains.

As both MtrF and UndA possess pseudo 2-fold symmetry between domains I,II and III,IV, we propose that MtrC and OmcA will also form a similar structure with 2-fold symmetry between the β-barrel and pentaheme domains. The conservation of this observed symmetry suggests that the *Shewanella* OMC family evolved from a common pentaheme ancestor. Gene duplication would have lead to the decameric structure observed in MtrF and predicted for MtrC and OmcA, whereas UndA would have evolved from this decameric family through the insertion of heme 7 into domain IV. UndA would thus represent the youngest known member of the *Shewanella* OMC family.

The ten heme staggered cross motif is conserved between MtrF and UndA, and the insertion of heme 7 within UndA does not affect the packing of hemes in this region. Heme 8, in particular, is completely conserved, with a mean least-squares value similar to those for the other hemes, showing that the positioning of heme 8 has not altered despite the addition of UndA heme 7. The distal ligand to UndA heme 7 is provided by His_{709}, whereas in MtrF the corresponding residue is Ala_{505}. This mutation significantly alters the arrangement of the surface loops in the two regions of MtrF and UndA as the conformation of the loop containing His_{709} is stabilized by the bonding between Heme 7 and His_{709}.

The significant rotation in the orientation of heme 5 between MtrF and UndA causes both the surface potential and heme exposure to significantly change. This change in exposure will significantly alter the properties of heme and could be due to the difference between the role of MtrF/MtrC as the terminal cytochromes of the MtrDEF/MtrCAB porin-cytochrome complexes, and the UndA/OmcA as satellite cytochromes. Thus MtrF heme 5 is exposed to allow interaction with MtrD, whereas UndA is protected by the polypeptide chain. The exposed MtrF heme 5 is likely to interact with insoluble metal oxides and soluble metal chelates in a significantly different way to the insulated UndA heme 5.

The outer membrane cytochromes of *Shewanella* are proposed to transfer electrons to the surface of extracellular electron acceptors, either through direct electron transfer, mediation by electron shuttles or by transfer to extracellular "nanowire" appendages (Shi et al., 2012). These cytochromes are known to be essential for effective electron transfer, but the biochemical mechanisms involved are poorly understood. It has never been determined whether outer membrane cytochromes act through nonspecific interactions with electron acceptors, or function as enzymes with localized areas for substrate binding and reduction. UndA has been previously shown to reduce both Fe(III)-citrate and Fe(III)-NTA with second order rate constants of 0.07 and 0.8 $\mu M^{-1}\ s^{-1}$ respectively (Shi et al., 2011). The structural data presented here shows that both Fe(III)-citrate trimer and Fe(III)-NTA dimer can associate close to heme 7, implicating this as a site of Fe(III)-chelate reduction.

Fe(III)-EDTA is known to be monomeric in solution, and was not observed to associate with the crystals of UndA. However, UndA reduces Fe(III)-EDTA with a measured second order rate constant >12.3 $\mu M^{-1}\ s^{-1}$, over 100 times faster than the observed rates for Fe(III)-citrate and Fe(III)-NTA (Shi et al., 2011). It is possible that the increased rate of UndA reduction is due to a less stable complex formed between UndA and Fe(III)-EDTA. Interestingly, the association of a single trimeric Fe(III)-citrate molecule may explain the observed polyphasic OMC oxidation, where $Fe(III)_3$-$(citrate)_3$ is reduced to $Fe(II)_3$-$(citrate)_3$ via Fe(II)-$Fe(III)_2$-$(citrate)_3$ and $Fe(II)_2$-Fe(III)-$(citrate)_3$. $Fe(III)_2$-$(NTA)_2$ would be reduced to $Fe(II)_2$-$(NTA)_2$ via Fe(III)-Fe(II)-$(NTA)_2$. The changes in conformation and redox potential of Fe(III)-chelates as they are systematically reduced by single electrons could account for the different phases during cytochrome oxidation.

The association of both Fe(III)-citrate and Fe(III)-NTA to the UndA surface near heme 7 suggests that reduction of soluble Fe(III) chelates could occur through interactions at this site on the protein surface, rather than through nonspecific reduction from multiple hemes across the cytochrome. The majority of heme containing active sites in other proteins such as NrfA or HAO are buried within the protein and are highly specific for small molecular substrates, whereas the area around heme 7 is highly solvent-exposed, making it unlikely to have specificity for individual substrates. Comparisons of native and chelate-bound structures of UndA reveal no significant difference in the position

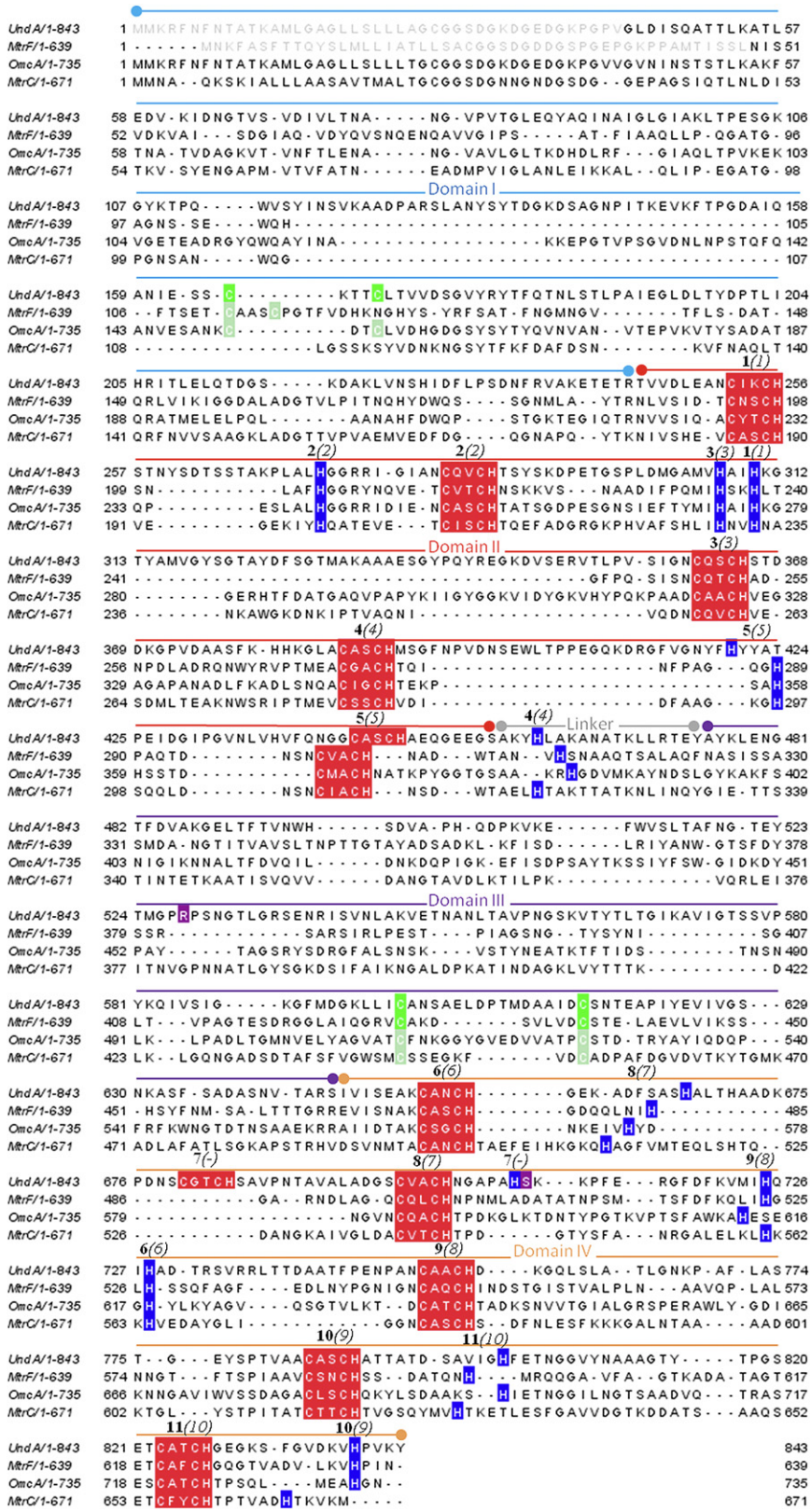

Figure 2. Structure-Based Amino Acid Alignment of Outer Membrane Cytochromes

The structures of UndA from *Shewanella sp.* HRCR-6 and MtrF from *S. oneidensis* were aligned using CCP4: SUPERPOSE to provide an amino acid alignment based on structural similarity. The sequences of MtrC and OmcA from *S. oneidensis* were then added to this alignment using MUSCLE (Edgar, 2004). Amino acids not observed in the crystal structures of MtrF or UndA are shown in light gray and the approximate amino acid regions that comprise each of the four domains are shown above the sequence. The CXXCH c-type cytochrome binding motifs for each sequence are highlighted in red with corresponding distal heme ligands highlighted in blue. The hemes and distal histidine from UndA (bold) or MtrF (italics in parenthesis) are numbered according to the position of the CXXCH motif in sequence and shown above each motif. Cysteines that form disulfide bonds in domains I and III are highlighted in green. Amino acid residues observed to associate with Fe(III)citrate or Fe(III)-NTA are highlighted in purple.

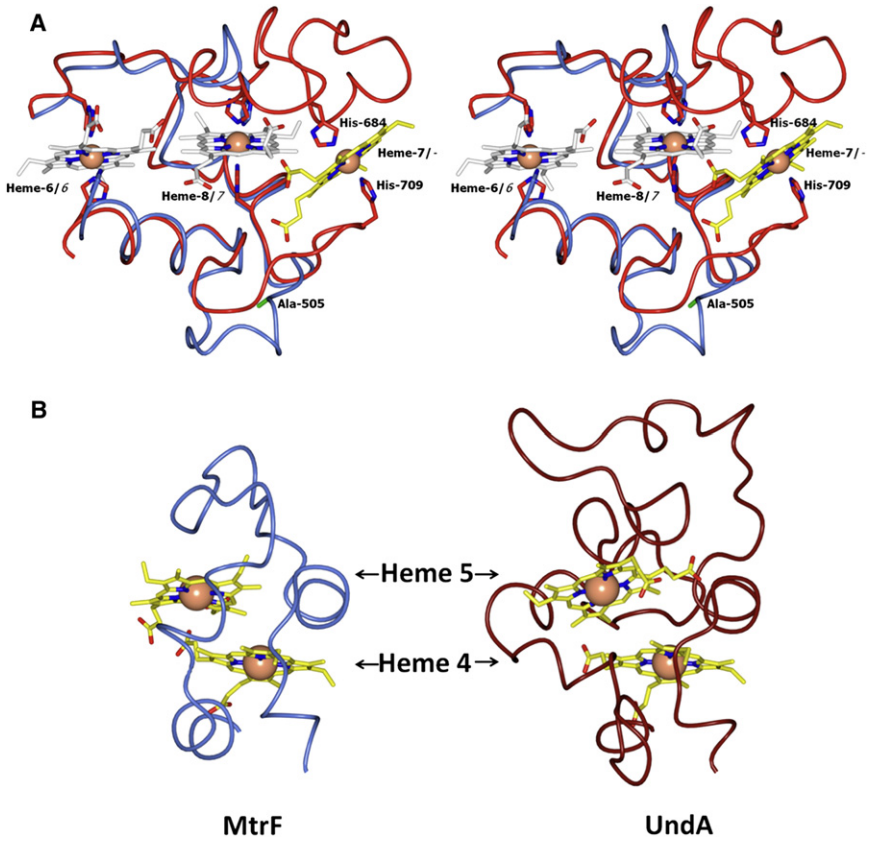

Figure 3. Comparison of UndA Heme 7 and Heme 5 with the Corresponding Regions of MtrF

(A) Stereo image of UndA hemes 6, 7, and 8 overlaid with the polypeptide backbone of MtrF. The UndA peptide chain is shown in red with heme 6, 8 represented as white sticks. The extra UndA heme 7 is in yellow with proximal and distal hemes labeled. The MtrF polypeptide chain is shown in blue and Ala_{505} carbons are shown as green sticks.

(B) Comparison of the region around heme 4 and 5 of MtrF (left) and UndA (right). The polypeptide chains of MtrF and UndA are displayed as ribbons and colored blue and red, respectively.

of side chains, and the B-factors of the polypeptide chain in this region are consistent with those of surrounding residues. The association of the soluble Fe(III)-chelates therefore appears to be facilitated by the overall positive charge of the heme 7 environment as opposed to an organized hydrogen bonding network. This overall positively charged surface results from the neutralization of the negatively charged propionate groups of hemes 7 and 8 by the side chains of arginine and lysine residues. This contrasts with the hemes of MtrF, where the exposed propionates generate a negatively charged surface over the deca-heme cross. We therefore propose that the region around heme 7 could be a rudimentary active site for association of soluble organic redox partners, which would be consistent with the UndA functioning as an enzyme with broad, but differential, specificity to a variety of substrates, in contrast to a nonspecific cathode on the cell surface.

EXPERIMENTAL PROCEDURES

Expression and Purification of UndA

The undA-encoding gene was amplified from *Shewanella* sp. Strain HRCR-6 and cloned into a pBAD202 (Invitrogen) plasmid. The undA gene was then mutated as described in Shi et al. (2011). The acetylation site was removed and UndA protein solubilized by mutating the DNA to give the plasmid pLS195, a soluble UndA construct where the 30 amino acids at the N-terminal were substituted with MSKKLLSVLFGASLAALALSPTAFAADQGG, and the C-terminal contained an insertion of KGELKLEGKPIPNPLLGLDSTRTGHHH HHH (Figure S1).

S. oneidensis MR-1 containing the pLS195 plasmid was grown aerobically at 30°C in Terrific Broth (TB) media containing 30 μg ml-1 kanamycin. Expression was induced by addition of 1 mM Arabinose at the mid-log phase of growth. Cells were grown overnight, harvested by centrifugation, and lysed using a French pressure cell. The crude extract was centrifuged in an ultracentrifuge at 186,000 × g to remove membranes and cell debris. The supernatant was loaded onto a 25 ml nickel charged Hi-trap NTA column pre-equilibrated with 20 mM Tris pH 7.8, 250 mM NaCl, 10 mM imidazole. The column was washed using 20 mM Tris pH 7.8, 250 mM NaCl, 30 mM imidazole. Fractions containing UndA were eluted in 20 mM Tris pH 7.8, 250 mM NaCl and a gradient of 30 to 100 mM imidazole over a volume of 100 ml.

Heme containing fractions were dialyzed into 20 mM Tris pH 7.8, 50 mM NaCl, and loaded onto a 5 ml Q-Sepharose column pre-equilibrated with 20 mM Tris pH 7.8, 50 mM NaCl. The Q-Sepharose column was washed with 20 mM Tris pH 7.8, 100 mM NaCl and fractions were collected using a gradient of 100–200 mM NaCl over 50 ml. Eluted fractions were analyzed by SDS-PAGE stained with Coomassie and UndA containing fractions were pooled and dialyzed into 20 mM Tris pH 7.8, 50 mM NaCl.

The dialyzed UndA fractions were loaded onto a Mono-Q 5/50 GL column equilibrated with 20 mM Tris pH 7.8, 50 mM NaCl. UndA was eluted with a NaCl gradient of 50 to 500 mM over 25 ml. Eluted fractions were analyzed using SDS-PAGE stained with Coomassie and UndA containing fractions were pooled and concentrated to 250 μl using a centrifugal concentrator. Finally the concentrated UndA was loaded onto an Superdex 200 10/300 GL gel filtration column pre-equilibrated with 50 mM Tris pH 7.0, 100 mM NaCl. Eluted fractions were analyzed using SDS-PAGE stained with Coomassie and fractions containing a single band corresponding to UndA were pooled and concentrated using a centrifugal concentrator to a final concentration of 8 mg ml^{-1}.

Crystallization and Data Collection

Crystals were obtained by vapor diffusion using either a 1:1 or 1:2 mixture of 8 mg/ml UndA in 50 mM HEPES pH 7.0 and a mother liquor comprising 0.1 M MES pH 6.5, 50 mM NaCl, 50 mM $MgCl_2$, 15% PEG 5000, 20% glycerol. Crystals were harvested into litholoops and flash-frozen in liquid nitrogen. Data were collected on frozen crystals at 100 K on beamlines I-02, I-04, I-041, and I-24 at the Diamond Light Source (UK). UndA crystals were of space group $P2_12_12_1$ with typical cell dimensions of a = 69.64 Å, b = 106.09 Å, and c = 151.65 Å. A SAD data set was collected at a wavelength of 1.72 Å to a final resolution of 3.4 Å. Further data sets from single crystals were collected using an X-ray wavelength of 0.97 Å. Crystals were soaked in mother liquor containing 10 mM Fe(III)-citrate or 10 mM Fe(III)-nitrilotriacetic acid for 10 min before harvesting. For the native data 25 mM 9,6 anthraquinone 2,6 disulfonate was added to the mother liquor as this was found to reduce nucleation, leading to larger crystals. Data sets were processed using XIA2, or MOSFLM and

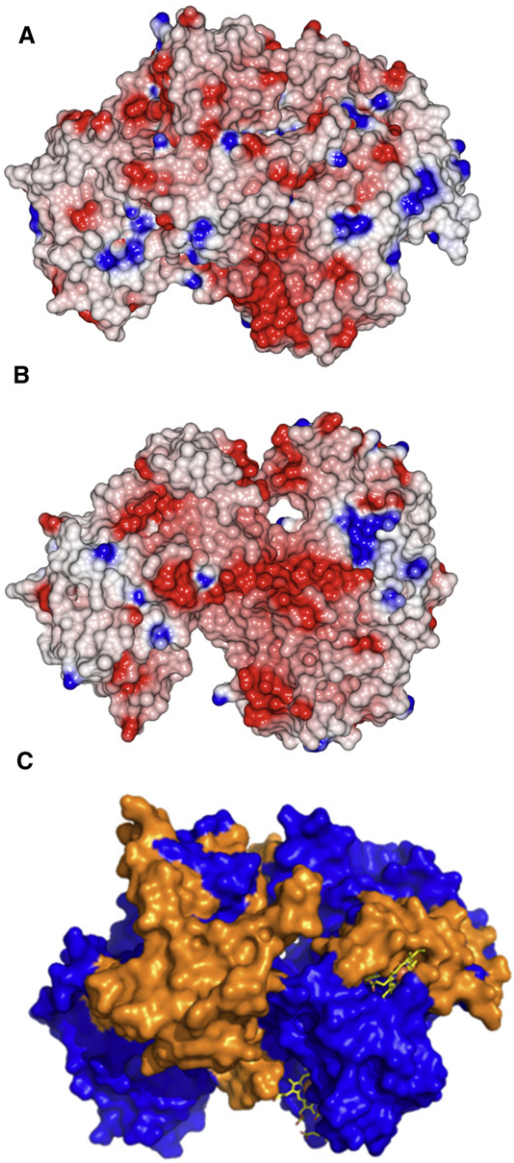

Figure 4. Comparison of the Electrostatic Surface Potential of MtrF and UndA

(A and B) The structures of UndA (A) and MtrF (B) were aligned using CCP4: SUPERPOSE and represented as electrostatic surface maps using the same scale and orientation. Maps were calculated using CCP4mg with potentials scaled from −0.5 V (red, negatively charged) to +0.5 (blue, positively charged). (C) Surface representation of UndA with the polypeptide chain colored blue. The nonconserved polypeptide inserts identified in Figure 2 are colored orange.

See also Figure S3.

SCALA as part of the CCP4 package and statistics are provided in Table 1 (Bailey, 1994; Leslie, 1999).

Structure Determination and Refinement

The SAD data set was analyzed using SHELX (Sheldrick, 2008). After processing using SHELXC and SHELXD a total of 11 iron atoms were identified in the asymmetric unit. Subsequent phasing was performed to a final resolution of 3.4 Å using SHELXE. Electron density maps calculated using these phases was sufficiently interpretable to manually place all 11 hemes, corresponding histidines and 70% of a polyalanine chain using COOT (Emsley and Cowtan, 2004).

Molecular replacement using PHASER (McCoy et al., 2007) was used to fit this model to a high resolution data set. The autobuild program ARPWARP (Morris et al., 2004) was then used to build residues 44–843 followed by alternating rounds of manual building and refinement using PHENIX (Adams et al., 2010) or REFMAC (Murshudov et al., 2011). Residues 1–44 and 854–874 were not observed in the electron density and were omitted from the final model. There were 22 residues (2.7%) in the generously allowed region and no residues in the disallowed region of the Ramachandran plot for the final UndA model structure.

Crystals soaked in 10 mM Fe(III)-citrate, Fe(III)-NTA, or Fe(III)-EDTA diffracted to resolutions of 2.17 Å, 2.10 Å, and 2.2 Å, respectively. The native UndA structure was used as model for molecular replacement and the F_O-F_C maps for the Fe(III)-citrate- and Fe(III)-NTA-soaked crystals showed unmodeled electron density corresponding to either trimeric Fe(III)-citrate or dimeric Fe(III)-NTA. No differences were observed in maps obtained from crystals soaked in Fe(III)-EDTA.

Fe(III) atoms and corresponding organic chelates were manually built into the models and refined for Fe(III)-citrate and Fe(III)-NTA. From these structures it is impossible to determine the oxidation state of the iron in either the hemes or the associated iron chelates, but in all structures the irons appear hexacoordinate, and we therefore assume these structures represent the oxidized form of iron.

ACCESSION NUMBERS

The refined coordinates for each structure have been deposited to the Protein Databank with accession numbers 3UCP (native UndA), 3UFH (Fe(III)-citrate UndA), and 3UFK (Fe(III)-NTA UndA).

SUPPLEMENTAL INFORMATION

Supplemental Information includes four figures and can be found with this article online at doi:10.1016/j.str.2012.04.016.

ACKNOWLEDGMENTS

This research was supported by the Biotechnology and Biological Sciences Research (H007288/1) and the Subsurface Biogeochemical Research program (SBR)/Office of Biological and Environmental Research (BER), U.S. Department of Energy (DOE), and is a contribution of the Pacific Northwest National Laboratory (PNNL) Scientific Focus Area. PNNL is operated for the DOE by Battelle under contract DE-AC05-76RLO 1830. D.J.R. is a Royal Society Wolfson Foundation Merit Award holder. T.C. is an RCUK fellow.

Received: February 1, 2012
Revised: March 31, 2012
Accepted: April 23, 2012
Published online: June 7, 2012

REFERENCES

Adams, P.D., Afonine, P.V., Bunkóczi, G., Chen, V.B., Davis, I.W., Echols, N., Headd, J.J., Hung, L.W., Kapral, G.J., Grosse-Kunstleve, R.W., et al. (2010). PHENIX: a comprehensive Python-based system for macromolecular structure solution. Acta Crystallogr. D Biol. Crystallogr. *66*, 213–221.

Bailey, S.; Collaborative Computational Project, Number 4. (1994). The CCP4 suite: programs for protein crystallography. Acta Crystallogr. D Biol. Crystallogr. *50*, 760–763.

Beliaev, A.S., and Saffarini, D.A. (1998). Shewanella putrefaciens mtrB encodes an outer membrane protein required for Fe(III) and Mn(IV) reduction. J. Bacteriol. *180*, 6292–6297.

Clarke, T.A., Edwards, M.J., Gates, A.J., Hall, A., White, G.F., Bradley, J., Reardon, C.L., Shi, L., Beliaev, A.S., Marshall, M.J., et al. (2011). Structure of a bacterial cell surface decaheme electron conduit. Proc. Natl. Acad. Sci. USA *108*, 9384–9389.

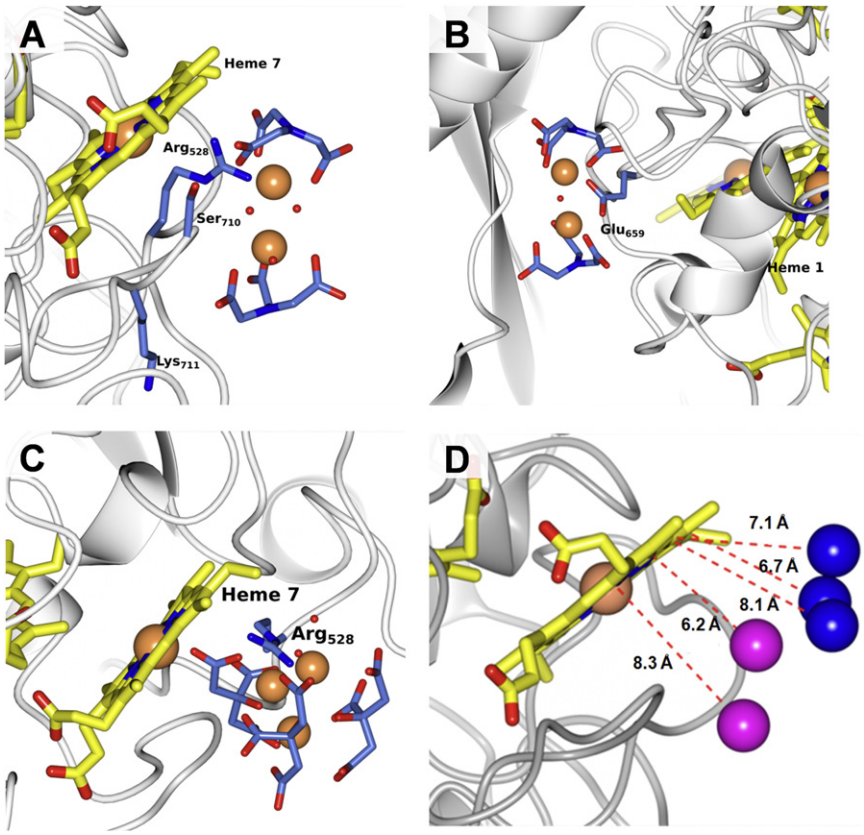

Figure 5. UndA in Complex with Fe(III)-NTA and Fe(III)citrate

The UndA backbone is represented in white cartoon format; iron atoms as orange spheres; heme porphyrin rings as yellow sticks; NTA and citrate molecules represented as blue sticks.

(A) Fe(III)-NTA dimer associated to UndA through interactions between NTA and the backbone amide groups of Ser_{710}, Lys_{711}, as well as the Arg_{528} guanidinium group. The backbones of Ser_{710} and Lys_{711} and Arg_{528} side chain are represented as blue sticks.

(B) Fe(III)-NTA dimer associated to UndA though hydrogen bonding interactions with Glu_{659}. The side chain of Glu_{659} is represented as blue sticks.

(C) Fe(III)citrate trimer associated to UndA through interactions between citrate and Arg_{528}, the Arg_{528} side chain is represented as blue sticks.

(D) The polypeptide chain and heme 7 of UndA with the iron atoms of Fe(III)-NTA (Pink) and Fe(III)-citrate (Blue). The distances between each iron atom and the porphyrin ring are shown.

See Figure S4.

Coursolle, D., and Gralnick, J.A. (2010). Modularity of the Mtr respiratory pathway of Shewanella oneidensis strain MR-1. Mol. Microbiol. *77*, 995–1008.

Coursolle, D., Baron, D.B., Bond, D.R., and Gralnick, J.A. (2010). The Mtr respiratory pathway is essential for reducing flavins and electrodes in Shewanella oneidensis. J. Bacteriol. *192*, 467–474.

Edgar, R.C. (2004). MUSCLE: a multiple sequence alignment method with reduced time and space complexity. BMC Bioinformatics *5*, 113.

Emsley, P., and Cowtan, K. (2004). Coot: model-building tools for molecular graphics. Acta Crystallogr. D Biol. Crystallogr. *60*, 2126–2132.

Fredrickson, J.K., Romine, M.F., Beliaev, A.S., Auchtung, J.M., Driscoll, M.E., Gardner, T.S., Nealson, K.H., Osterman, A.L., Pinchuk, G., Reed, J.L., et al. (2008). Towards environmental systems biology of Shewanella. Nat. Rev. Microbiol. *6*, 592–603.

Hartshorne, R.S., Jepson, B.N., Clarke, T.A., Field, S.J., Fredrickson, J., Zachara, J., Shi, L., Butt, J.N., and Richardson, D.J. (2007). Characterization of Shewanella oneidensis MtrC: a cell-surface decaheme cytochrome involved in respiratory electron transport to extracellular electron acceptors. J. Biol. Inorg. Chem. *12*, 1083–1094.

Hartshorne, R.S., Reardon, C.L., Ross, D., Nuester, J., Clarke, T.A., Gates, A.J., Mills, P.C., Fredrickson, J.K., Zachara, J.M., Shi, L., et al. (2009). Characterization of an electron conduit between bacteria and the extracellular environment. Proc. Natl. Acad. Sci. USA *106*, 22169–22174.

Heath, S.L., Powell, A.K., Utting, H.L., and Helliwell, M. (1992). Crystal and molecular-structure of a new mu-oxo-bridged iron(iii) dimer formed with the nitrilotriacetate ligand. J. Chem. Soc. Dalton Trans. 305–307.

Johs, A., Shi, L., Droubay, T., Ankner, J.F., and Liang, L. (2010). Characterization of the decaheme c-type cytochrome OmcA in solution and on hematite surfaces by small angle x-ray scattering and neutron reflectometry. Biophys. J. *98*, 3035–3043.

Leslie, A.G.W. (1999). Integration of macromolecular diffraction data. Acta Crystallogr. D Biol. Crystallogr. *55*, 1696–1702.

Lower, B.H., Shi, L., Yongsunthon, R., Droubay, T.C., McCready, D.E., and Lower, S.K. (2007). Specific bonds between an iron oxide surface and outer membrane cytochromes MtrC and OmcA from Shewanella oneidensis MR-1. J. Bacteriol. *189*, 4944–4952.

Lower, B.H., Yongsunthon, R., Shi, L., Wildling, L., Gruber, H.J., Wigginton, N.S., Reardon, C.L., Pinchuk, G.E., Droubay, T.C., Boily, J.F., and Lower, S.K. (2009). Antibody recognition force microscopy shows that outer membrane cytochromes OmcA and MtrC are expressed on the exterior surface of Shewanella oneidensis MR-1. Appl. Environ. Microbiol. *75*, 2931–2935.

McCoy, A.J., Grosse-Kunstleve, R.W., Adams, P.D., Winn, M.D., Storoni, L.C., and Read, R.J. (2007). Phaser crystallographic software. J. Appl. Cryst. *40*, 658–674.

McLean, J.S., Pinchuk, G.E., Geydebrekht, O.V., Bilskis, C.L., Zakrajsek, B.A., Hill, E.A., Saffarini, D.A., Romine, M.F., Gorby, Y.A., Fredrickson, J.K., and Beliaev, A.S. (2008). Oxygen-dependent autoaggregation in Shewanella oneidensis MR-1. Environ. Microbiol. *10*, 1861–1876.

Morris, R.J., Zwart, P.H., Cohen, S., Fernandez, F.J., Kakaris, M., Kirillova, O., Vonrhein, C., Perrakis, A., and Lamzin, V.S. (2004). Breaking good resolutions with ARP/wARP. J. Synchrotron Radiat. *11*, 56–59.

Murshudov, G.N., Skubák, P., Lebedev, A.A., Pannu, N.S., Steiner, R.A., Nicholls, R.A., Winn, M.D., Long, F., and Vagin, A.A. (2011). REFMAC5 for the refinement of macromolecular crystal structures. Acta Crystallogr. D Biol. Crystallogr. *67*, 355–367.

Pitts, K.E., Dobbin, P.S., Reyes-Ramirez, F., Thomson, A.J., Richardson, D.J., and Seward, H.E. (2003). Characterization of the Shewanella oneidensis MR-1 decaheme cytochrome MtrA: expression in Escherichia coli confers the ability to reduce soluble Fe(III) chelates. J. Biol. Chem. *278*, 27758–27765.

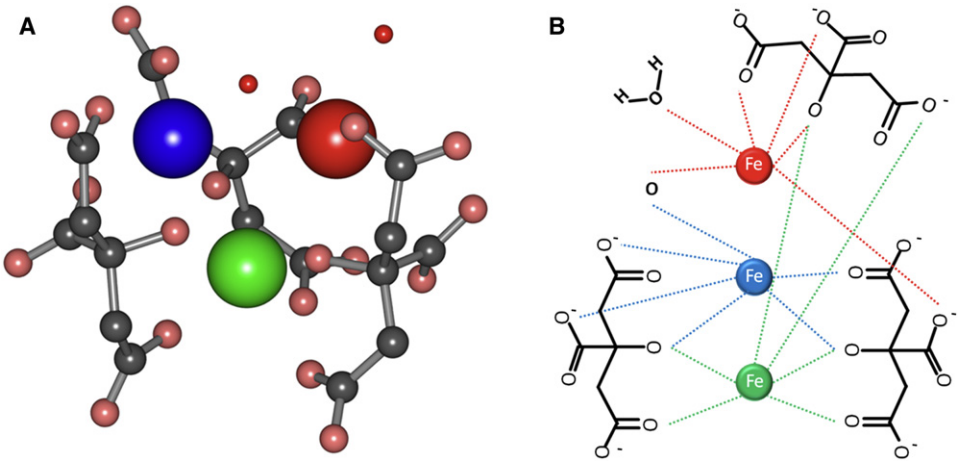

Figure 6. Conformation of the Bound Fe(III)-Citrate

(A) Structure of the experimentally determined Fe(III)-citrate trimer. The three iron atoms are displayed as large spheres colored red, green, and blue. The citrate molecules are displayed as sticks with carbons colored gray and the associated water and oxo-bridge displayed as small red spheres.

(B) Schematic representation of the structural organization of the Fe(III)-citrate trimer associated with UndA. Iron atoms are colored according to the corresponding iron atom in (A). Bonds are colored according to originating iron atom.

Ross, D.E., Ruebush, S.S., Brantley, S.L., Hartshorne, R.S., Clarke, T.A., Richardson, D.J., and Tien, M. (2007). Characterization of protein-protein interactions involved in iron reduction by Shewanella oneidensis MR-1. Appl. Environ. Microbiol. *73*, 5797–5808.

Ross, D.E., Brantley, S.L., and Tien, M. (2009). Kinetic characterization of OmcA and MtrC, terminal reductases involved in respiratory electron transfer for dissimilatory iron reduction in Shewanella oneidensis MR-1. Appl. Environ. Microbiol. *75*, 5218–5226.

Sharma, S., Cavallaro, G., and Rosato, A. (2010). A systematic investigation of multiheme c-type cytochromes in prokaryotes. J. Biol. Inorg. Chem. *15*, 559–571.

Sheldrick, G.M. (2008). A short history of SHELX. Acta Crystallogr. A *64*, 112–122.

Shi, L., Chen, B., Wang, Z., Elias, D.A., Mayer, M.U., Gorby, Y.A., Ni, S., Lower, B.H., Kennedy, D.W., Wunschel, D.S., et al. (2006). Isolation of a high-affinity functional protein complex between OmcA and MtrC: Two outer membrane decaheme c-type cytochromes of Shewanella oneidensis MR-1. J. Bacteriol. *188*, 4705–4714.

Shi, L., Belchik, S.M., Wang, Z.M., Kennedy, D.W., Dohnalkova, A.C., Marshall, M.J., Zachara, J.M., and Fredrickson, J.K. (2011). Identification and characterization of UndAHRCR-6, an outer membrane endecaheme c-type cytochrome of Shewanella sp. strain HRCR-6. Appl. Environ. Microbiol. *77*, 5521–5523.

Shi, L., Rosso, K.M., Clarke, T.A., Richardson, D.J., Zachara, J., and Fredrickson, J. (2012). Molecular underpinnings of Fe(III) oxide reduction by Shewanella Oneidensis MR-1. Front. Microbiol. *3*, 50.

Silva, A.M.N., Kong, X., Parkin, M.C., Cammack, R., and Hider, R.C. (2009). Iron(III) citrate speciation in aqueous solution. Dalton Trans. (40), 8616–8625.

Xiong, Y.J., Shi, L., Chen, B.W., Mayer, M.U., Lower, B.H., Londer, Y., Bose, S., Hochella, M.F., Fredrickson, J.K., and Squier, T.C. (2006). High-affinity binding and direct electron transfer to solid metals by the Shewanella oneidensis MR-1 outer membrane c-type cytochrome OmcA. J. Am. Chem. Soc. *128*, 13978–13979.

Wang, Z.M., Liu, C.X., Wang, X.L., Marshall, M.J., Zachara, J.M., Rosso, K.M., Dupuis, M., Fredrickson, J.K., Heald, S., and Shi, L. (2008). Kinetics of reduction of Fe(III) complexes by outer membrane cytochromes MtrC and OmcA of Shewanella oneidensis MR-1. Appl. Environ. Microbiol. *74*, 6746–6755.

